Canadian Science Publishing | Canadian Journal of Physics

Effect of nonlinear temperature and concentration profiles on the stability of a layer of fluid with chemical reaction

Journal:	*Canadian Journal of Physics*
Manuscript ID	cjp-2020-0302.R1
Manuscript Type:	Article
Date Submitted by the Author:	16-Aug-2020
Complete List of Authors:	Mahajan, Amit; National Institute of Technology Delhi, Department of Applied Sciences Tripathi, Vinit Kumar; National Institute of Technology Delhi, Department of Applied Sciences
Keyword:	convection, Nonlinear Stability, Chemical Reaction, Temperature and Concentration Profiles, Double Diffusion
Is the invited manuscript for consideration in a Special Issue? :	Not applicable (regular submission)

Effect of nonlinear temperature and concentration profiles on the stability of a layer of fluid with chemical reaction

Amit Mahajan and Vinit Kumar Tripathi

Department of Applied Sciences, National Institute of Technology Delhi, India 110040
Email: amitmahajan2006@gmail.com, ankittripathi10892@gmail.com

Abstract

Investigation of the onset of thermosolutal convection with chemical reaction is carried out for different types of basic temperature and concentration gradients using linear theory and energy method. An unconditional non-linear stability with exponential decay of finite amplitude perturbations is achieved and the Galerkin technique is utilized to solve the resulting Eigen-value problem obtained from linear and non-linear analysis. The numerical scheme is validated with existing results and the results are obtained for linear, parabolic, inverted parabolic, piecewise linear, oscillatory and step-function profiles of temperature and concentration gradients. The linear and non-linear results show the existence of subcritical instability.

1. Introduction

In the standard Bénard problem [1] the instability is driven by a temperature difference between the upper and lower planes bounding the fluid. If the fluid layer additionally has salt dissolved in it then there are potentially two destabilizing sources for the density difference, the temperature field and salt field. When there are two effects such as this, the phenomenon of convection that arises is termed as double-diffusive convection [2]. Natural Convection where the buoyancy is driven by both temperature and some dissolved material is necessary in order to understand the development of a number of systems that are influenced due to density variation of fluid. The study of thermosolutal convection earlier helped in the understanding of the phenomenon of convection that occurs in magma chamber and in sun (where heat and helium diffuses). Later, the study attained great importance in a wide range of applications in industry and geophysics such as extraction of oil from underground reservoirs, the modelling of packed sphere beds, in polymer solutions and lubricants, flows in fuel cells, underground disposal of nuclear wastes, oceanography and in manufacturing the different type of articles which are useful in aircraft and automobile industry.

In thermosolutal convection solute may either dissolve in fluid or take form of precipitate and hence the concept of chemical reaction generates here i.e. dissolved mineral can react with fluid on heating and influence the onset of convection. Wollkind and Frisch [3] studied reactive effects on convection in a horizontal layer of dissociating fluid. They used normal mode technique for linear analysis and showed that for a non-reactive fluid layer heated from below, slight departure occurs on the onset of convection from the classical Bénard problem. This linear perturbation problem was extended by Wollkind and Frisch [4] to include a nonlinear stability analysis of a horizontal layer of dissociating fluid, heated from above or below. The linear and non-linear analysis for a chemically driven convection model is performed by Bdzil and Frisch [5, 6]. Krusin and Ross [7] studied the Rayleigh Bénard instability in the binary fluids and later, Gitterman and Steinberg [8] studied the convective instabilities in reactive fluid with fast chemical reaction. Steinberg and Brand [9] discussed the effect of chemical reaction on the onset of convection in a porous medium. They ignored the effect of thermal diffusion on the stability of fluid assuming that it is less effective on the onset of convection than that of chemical reaction. The work was extended by Pritchard and Richardson [10] to include the effect of fast as well as slow chemical reaction on the instability of fluid and analyzed the effect of solutal diffusion on the stability of flow. Pritchard and Richardson's [10] work was further extended by Wang and Tan [11] for Darcy-Brinkman model in a sparsely packed porous medium using linear stability theory and they reported the behavior of Darcy number, Lewis number and reaction term on the onset of thermosolutal convection. Srivastava and Bera [12] used linear and weak non-linear analysis to show the effect of chemical reaction on stability of thermosolutal convection of non-Newtonian couple stress fluid. Malashetty and Biradar [13] applied the linear and nonlinear stability analysis to analyze the effect of chemical reaction on thermosolutal convection in anisotropic porous layer. In [12,13] the normal mode technique for the linear stability analysis and to obtain finite amplitude Rayleigh number a truncated two term Fourier series method is used. Al-Sulaimi [14] studied the thermosolutal convection with reaction in a porous medium of Darcy type using linear and nonlinear method. He used Chebyshev tau method to obtain the stability and instability results for the system heated below and salted above as well as for the system heated and salted from below. Al-Sulaimi [15] extended this work and studied the energy stability of Brinkman model for thermosolutal convection with chemical reaction. He showed the effect of Brinkman number, chemical reaction on the onset of convection for the two cases when the system is salted below and heated below

and for the system salted above and heated below. Recently, Harfash and Meften [16] used linear instability analysis, non-linear stability analysis, and weighted energy analysis to show the effect of couple stresses and chemical reaction on the onset of thermosolutal convection of reactive fluid. Some aspects of stability are discussed by Makinde and coworkers [17-20].

Graham [21] and Chandra [22] observed from their experiment that in thin layers a form of convection occurs at Rayleigh number less than that predicted by linear theory. Sutton [23] noted that the likely explanation of this phenomenon was the non-uniformity of temperature gradient in such layers. Sparrow et al. [24] deduced the effect of parabolic basic temperature profile on the onset of convection. Homsy [25] studied the global stability of time dependent profile using energy method and further Currie [26] showed the effect of piecewise linear temperature profile on the onset of convection and he observed that convection occurs much faster for this profile as compared to the linear profile. Nield [27] used linear stability analysis to examine the stability of horizontal fluid layer in case of non-uniform temperature gradient and applied single order Galerkin technique to find the stability boundary. He observed that when basic thermal gradient is nowhere negative the largest instability occurs in case when basic temperature profile is of the form of a Dirac-delta function. Further, the effect of non-uniform temperature gradient on the onset of convection in fluid saturated porous media is investigated by Rudraiah et al. [28] and they made a comparison between the critical Rayleigh number obtained for isothermal and adiabatic boundary and observed that convection occurs early in the case of adiabatic boundary than that of isothermal boundary. Effect of non-uniform temperature gradient on the onset of convection driven by buoyancy force in couple stress fluid saturated porous medium is discussed by Shivakumara [29].

In the present work, the linear analysis using normal mode technique and non-linear analysis using energy method is carried out to analyze the onset of convection in a fluid layer having chemically reacting salt dissolved in it. An unconditional energy decay is obtained in the nonlinear analysis. The numerical results for the linear and non-linear theory obtained by Galerkin technique show the possibility of existence of subcritical instability for the linear, parabolic, inverted parabolic, piecewise linear, oscillatory profile and stepwise function profiles of temperature and concentration gradients considered in the present work. The behavior of solute and chemical reaction parameters is also analyzed.

2. Mathematical formulation of the problem

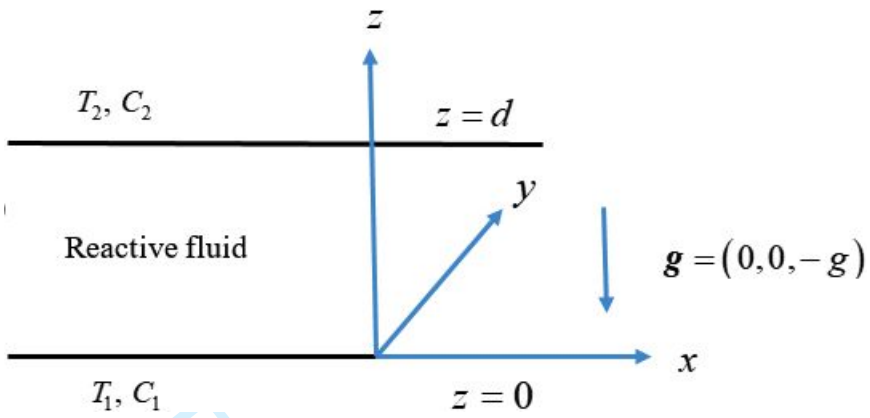

Figure 1 Physical configuration of the problem

Let us consider an incompressible fluid of thickness d bounded by two infinite parallel planes, and let $\Delta T = T_1 - T_2$ & $\Delta C = C_1 - C_2$ be the temperature and concentration differences respectively, maintained between these two planes. Cartesian axes are taken with x-axis along the lower plane and y-axis is infinitely extended perpendicular to x-axis and z-axis where z-axis is vertically upward and gravity $\boldsymbol{g}$ acts in negative z-direction. Under the Boussinesq approximation the governing equations for flow are as follows

$$\nabla \cdot \boldsymbol{q} = 0 \tag{1}$$

$$\rho\left(\frac{\partial \boldsymbol{q}}{\partial t} + \boldsymbol{q}\cdot\nabla\boldsymbol{q}\right) = -\nabla p + \mu\nabla^2\boldsymbol{q} + k_i g\rho\alpha_T T - k_i g\rho\alpha_C C \tag{2}$$

The transport of heat and solute is described by the advection-diffusion equations

$$\frac{\partial T}{\partial t} + \boldsymbol{q}\cdot\nabla T = k_T\nabla^2 T \tag{3}$$

$$\frac{\partial C}{\partial t} + \boldsymbol{q}\cdot\nabla C = k_C\nabla^2 C + \hat{k}\left[S_0 + S_1\left(T - T_0\right) - C\right] \tag{4}$$

where $\rho, \boldsymbol{q}, p, \mu, t, T, C, \alpha_T, \alpha_C, k_T, k_C$ are the density, velocity, pressure, fluid viscosity, time, temperature, mass concentration, coefficient of thermal expansion, coefficient of solute expansion, thermal diffusivity and solute diffusivity respectively, $k_i = (0,0,1)$ is the unit vector. Following

the work of Gitterman and Steinberg [8], Pritchard and Richardson [10], $S_0 + S_1(T - T_0) = C_{eq}(T)$ where S_0, S_1, T_0 are constants and $\hat{k} > 0$ is the reaction coefficient.

In the quiescent state, the temperature and concentration distribution is freezed at any instant of time using quasi-static approximation (see Currie [26]) which allows us to write the conduction solution as

$$\boldsymbol{q} = \boldsymbol{q}_b = \mathbf{0},\ p = p_b(z),\ f_T(z) = (-d/\Delta T)\frac{dT_b}{dz},\ f_C(z) = (-d/\Delta C)\frac{dC_b}{dz} \tag{5}$$

where subscript b denotes the basic state and $f_T(z),\ f_C(z)$ are non-dimensional temperature and salt gradients respectively, satisfying

$$\int_0^1 f_T(z)\,dz = 1\ ,\ \int_0^1 f_C(z)\,dz = 1$$

It is assumed that the instability occurs by way of perturbation to the conduction solution. On considering the perturbations to conduction state (5) in the form

$$\boldsymbol{q} = \boldsymbol{q}_b(z) + \boldsymbol{q}',\ p = p_b(z) + p',\ \rho = \rho_b(z) + \rho',\ T = T_b(z) + \theta,\ C = C_b(z) + \phi \tag{6}$$

where $\boldsymbol{q}' = (u, v, w), p', \rho', \theta, \phi$ are perturbed velocity, pressure, density, temperature, and concentration respectively, the conservation equations (1)-(4) take the form (on dropping the primes)

$$\rho\left(\frac{\partial \boldsymbol{q}}{\partial t} + \boldsymbol{q}\cdot\nabla\boldsymbol{q}\right) = -\nabla p + \mu\nabla^2\boldsymbol{q} + k_i g\rho\alpha_T\theta - k_i g\rho\alpha_C\phi \tag{7}$$

$$\nabla\cdot\boldsymbol{q} = 0 \tag{8}$$

$$\frac{\partial\theta}{\partial t} + \boldsymbol{q}\cdot\nabla\theta = k_T\nabla^2\theta - w\frac{\partial T_b}{\partial z} \tag{9}$$

$$\frac{\partial\phi}{\partial t} + \boldsymbol{q}\cdot\nabla\phi = k_C\nabla^2\phi - w\frac{\partial C_b}{\partial z} + \hat{k}S_1\theta - \hat{k}\phi \tag{10}$$

The system (7) -(10) is non-dimensionalized using suitable scales given by

$$z = dz^*,\ \boldsymbol{q} = \frac{k_T}{d}\boldsymbol{q}^*, t = \frac{d^2}{k_T}t^*, p = \frac{\mu k_T}{d^2}p^*,\ \theta = \frac{\Delta T}{\left(R^{1/2}\right)}\theta^*, \phi = \frac{\Delta C}{\left(Rs^{1/2}\right)}\phi^*$$

and the dimensionless perturbed system of equations (after dropping the asterisks) is written as

$$\frac{1}{\mathrm{Pr}}\left(\frac{\partial\boldsymbol{q}}{\partial t} + \boldsymbol{q}\cdot\nabla\boldsymbol{q}\right) = -\nabla p + \nabla^2\boldsymbol{q} + \left(R^{1/2}\right)k_i\theta - \left(Rs^{1/2}\right)k_i\phi \tag{11}$$

$$\nabla\cdot\boldsymbol{q} = 0 \tag{12}$$

$$\frac{\partial \theta}{\partial t} + \boldsymbol{q}\cdot\nabla\theta = \nabla^2\theta + f_T(z)\left(R^{1/2}\right)w \tag{13}$$

$$Le\left(\frac{\partial \phi}{\partial t} + \boldsymbol{q}\cdot\nabla\phi\right) = \nabla^2\phi + f_C(z)\left(Rs^{1/2}\right)w + h\theta - \eta\phi \tag{14}$$

where $Le = \frac{k_T}{k_C}$ is Lewis number, $\Pr = \frac{\mu}{\rho k_T}$ is Prandtl number, $R = \frac{d^3 g\rho\alpha_T \Delta T}{\mu k_T}$ is thermal Rayleigh number, $Rs = \frac{d^3 g\rho\alpha_C \Delta C}{\mu k_C}$ is Solutal Rayleigh number and $h = \hat{k}\, d^2 S_1 \sqrt{\frac{\alpha_C \Delta T}{k_C \alpha_T \Delta C k_T}}$, $\eta = \frac{\hat{k}\, d^2}{k_C}$ are chemical reaction parameters.

The boundary conditions for the system of equations (11) -(14) are as follows

$$w = \frac{dw}{dz} = \theta = \phi = 0 \text{ at } z = 0,1 \tag{15}$$

3. Linear stability analysis

Linear analysis is performed by considering the perturbations given in (6) to be infinitesimally small and so the quadratic and higher order terms in equations (11) -(14) are neglected [see, Chandrasekhar [1]]. The normal mode solution is chosen after removing pressure term from (11) in the form $(\boldsymbol{q},\theta,\phi) = [\boldsymbol{q}(z),\Theta(z),\Phi(z)]\exp\left[i\left(a_x x + a_y y\right) + \sigma t\right]$, with $a = \sqrt{a_x^{\,2} + a_y^{\,2}}$, as the wave number of disturbance and σ the growth rate. Letting $D = \frac{d}{dz}$, leads to following system of linear equations

$$\frac{\sigma}{\Pr}(D^2 - a^2)W = (D^2 - a^2)^2 W - \left(R^{1/2}\right)a^2\Theta + \left(Rs^{1/2}\right)a^2\Phi \tag{16}$$

$$\sigma\Theta = (D^2 - a^2)\Theta + \left(R^{1/2}\right)f_T(z)W \tag{17}$$

$$Le\sigma\Phi = (D^2 - a^2)\Phi + \left(Rs^{1/2}\right)f_C(z)W + h\Theta - \eta\Phi \tag{18}$$

with the boundary conditions (15) take the form

$$W = DW = \Theta = \Phi = 0 \text{ at } z = 0,1 \tag{19}$$

Equations (16) -(18) together with boundary condition (19) form eigenvalue problem, which is solved using Galerkin method. To this end, let us consider the unknown variables as

$$W = \sum_{i=1}^{N} A_i W_i,\ \Theta = \sum_{i=1}^{N} B_i\Theta_i,\ \Phi = \sum_{i=1}^{N} C_i\Phi_i \tag{20}$$

where W_i, Θ_i, Φ_i are basis functions, chosen in such a way that the boundary conditions are satisfied and A_i, B_i, C_i are constants. On Substituting (20) into the stationary form of the system of equations (16)-(18) and multiplying to the resultant equations by W_j, Θ_j, Φ_j respectively and performing the integration with respect to z, between $z = 0$ and $z = 1$ and using boundary condition (19) provides a system of linear homogeneous algebraic equations as below

$$X_{1ji}A_i + X_{2ji}B_i + X_{3ji}C_i = 0$$

$$Y_{1ji}A_i + Y_{2ji}B_i + Y_{3ji}C_i = 0 \qquad (21)$$

$$P_{1ji}A_i + P_{2ji}B_i + P_{3ji}C_i = 0$$

The coefficients X_{1ji} to P_{3ji} contains inner product of the basis function, given by

$$X_{1ji} = \left\langle D^2W_jD^2W_i + a^4W_jW_i + 2a^2DW_jDW_i \right\rangle$$

$$X_{2ji} = \left\langle -R^{1/2}a^2W_j\Theta_i \right\rangle$$

$$X_{3ji} = \left\langle Rs^{1/2}a^2W_j\Phi_i \right\rangle$$

$$Y_{1ji} = \left\langle R^{1/2}f_T(z)\Theta_jW_i \right\rangle$$

$$Y_{2ji} = \left\langle -D\Theta_jD\Theta_i - a^2\Theta_j\Theta_i \right\rangle$$

$$Y_{3ji} = 0 \qquad (22)$$

$$P_{1ji} = \left\langle Rs^{1/2}\, f_C(z)\Phi_jW_i \right\rangle$$

$$P_{2ji} = \left\langle h\Phi_j\Theta_i \right\rangle$$

$$P_{3ji} = \left\langle -D\Phi_jD\Phi_i - a^2\Phi_j\Phi_i - \eta\Phi_j\Phi_i \right\rangle$$

Here the inner product is defined as $\langle ... \rangle = \int_0^1 (...)dz$.

The above set of equations, given by (21), contain a non-trivial solution if and only if

$$\begin{vmatrix} X_{1ji} & X_{2ji} & X_{3ji} \\ Y_{1ji} & Y_{2ji} & Y_{3ji} \\ P_{1ji} & P_{2ji} & P_{3ji} \end{vmatrix} = 0 \tag{23}$$

Now, we choose the following trial functions

$$W_i = (z^{i+3} - 2z^{i+2} + z^{i+1})T^*_{i-1}$$

$$\Theta_i = (z^i - z^{i+1})T^*_{i-1}$$

$$\Phi_i = (z^i - z^{i+1})T^*_{i-1}$$

where T_i^*'s are modified Chebyshev polynomials. The critical Rayleigh number of linear theory $R_{cL} = \min_{a>0} R(a)$ is calculated numerically and the results are presented in section 5.

4. Nonlinear stability analysis

Now, the perturbations in (6) are assumed to be finite and so the non-linear terms in the system (11) -(14) are retained. This non-linear system is now solved by energy method, which is well described in Straughan [30]. To begin with, we multiply (11) by $\boldsymbol{q}$, (13) by θ, and (14) by ϕ, and integrate over the periodic cell V (using boundary condition (15) and application of Divergence theorem) to obtain the following system of equations

$$\frac{1}{2\,\mathrm{Pr}}\frac{d}{dt}\|\boldsymbol{q}\|^2 = -\|\nabla \boldsymbol{q}\|^2 + R^{1/2}\langle \theta w\rangle - Rs^{1/2}\langle \phi w\rangle \tag{25}$$

$$\frac{1}{2}\frac{d}{dt}\|\theta\|^2 = -\|\nabla \theta\|^2 + R^{1/2}\langle f_T(z)\theta w\rangle \tag{26}$$

$$\frac{Le}{2}\frac{d}{dt}\|\phi\|^2 = -\|\nabla \phi\|^2 + Rs^{1/2}\langle f_C(z) w\phi\rangle + h\langle \phi\theta\rangle - \eta\|\phi\|^2 \tag{27}$$

where $\|\cdot\|$ denotes the $L^2(V)$ norm and $\langle\cdot\rangle$ denotes the integration. Using the concept of coupling parameters (Joseph [31]), energy functional $E(t)$ is constructed (with λ_1, λ_2 as coupling parameters) as

$$E(t) = \frac{1}{2\,\mathrm{Pr}}\|\boldsymbol{q}\|^2 + \frac{\lambda_1}{2}\|\theta\|^2 + \frac{\lambda_2 Le}{2}\|\phi\|^2 \tag{28}$$

The evolution of energy with respect to time is

$$\frac{dE(t)}{dt} = \frac{1}{2\,\mathrm{Pr}}\frac{d}{dt}\|\boldsymbol{q}\|^2 + \frac{\lambda_1}{2}\frac{d}{dt}\|\theta\|^2 + \frac{\lambda_2 Le}{2}\frac{d}{dt}\|\phi\|^2 \tag{29}$$

Substituting (25) -(27) in (29), we may write

$$\frac{dE(t)}{dt} = I - D \tag{30}$$

where $I = R^{1/2}\langle\theta w\rangle - Rs^{1/2}\langle\phi w\rangle + \lambda_1 R^{1/2}\langle f_T(z) w\theta\rangle + \lambda_2 Rs^{1/2}\langle f_C(z) w\phi\rangle + \lambda_2 h\langle\theta\phi\rangle$ contains non-definite production terms and $D = \|\nabla \boldsymbol{q}\|^2 + \lambda_1\|\nabla\theta\|^2 + \lambda_2\|\nabla\phi\|^2 + \lambda_2\eta\|\phi\|^2$ consists of positive definite dissipation terms.

Setting

$$\frac{1}{R_E} = \max_H \frac{I}{D} \tag{31}$$

where H is space of admissible solution, then we require $R_E > 1$ so that $b_1 = \left(1 - \frac{1}{R_E}\right) > 0$ and (30) may be written as

$$\frac{dE}{dt} \le -b_1 D \tag{32}$$

Using Poincare's inequality the dissipation terms D are

$$D \ge \frac{2\pi^2}{2}[\Pr\|\boldsymbol{q}\|^2 + \lambda_1\|\theta\|^2 + \lambda_2 Le\|\phi\|^2] \ge 2\pi^2 k' E \tag{33}$$

where $k' = \min\left\{1, \Pr, \frac{1}{Le}\right\}$.

The equation (32) using (33) is written as

$$\frac{dE}{dt} \le -2\pi^2 k' b_1 E$$

Integrating above equation, we obtain

$$E(t) \le E(0)\exp\left(-2\pi^2 k' b_1 t\right)$$

It ensures that energy decays exponentially fast for all values of $E(0)$ and yield unconditional nonlinear stability.

Now, the variational problem (31) gives the nonlinear energy threshold, the associated Euler Lagrange's equations after taking transformation $\theta = \frac{\hat{\theta}}{\sqrt{\lambda_1}}, \phi = \frac{\hat{\phi}}{\sqrt{\lambda_2}}$ are obtained using the calculus of variation and these are written as

$$2\nabla^2 \boldsymbol{q} + \frac{R^{1/2}\theta k_i}{\sqrt{\lambda_1}} - \frac{Rs^{1/2}\phi k_i}{\sqrt{\lambda_2}} + \sqrt{\lambda_1} R^{1/2} f_T(z)\theta k_i + \sqrt{\lambda_2} Rs^{1/2} f_C(z)\phi k_i = -\nabla p \tag{34}$$

$$2\nabla^2\theta+\frac{R^{1/2}}{\sqrt{\lambda_1}}w+\sqrt{\lambda_1}R^{1/2}f_T(z)w+\sqrt{\frac{\lambda_2}{\lambda_1}}h\phi=0 \tag{35}$$

$$2\nabla^2\phi-2\eta\phi-\frac{Rs^{1/2}}{\sqrt{\lambda_2}}w+\sqrt{\lambda_2}Rs^{1/2}f_C(z)w+\sqrt{\frac{\lambda_2}{\lambda_1}}h\theta=0 \tag{36}$$

where p is Lagrange multiplier. Applying the double curl on equation (34) and taking the third component of resulting equation, reduces it to the following

$$2\nabla^4 w-\frac{R^{1/2}}{\sqrt{\lambda_1}}a^2\theta+\frac{Rs^{1/2}}{\sqrt{\lambda_2}}a^2\phi-\sqrt{\lambda_1}R^{1/2}f_T(z)a^2\theta-\sqrt{\lambda_2}Rs^{1/2}f_C(z)a^2\phi=0 \tag{37}$$

Now we assume, a plane tiling form $(w,\theta,\phi)=(W,\Theta,\Phi)U(x,y)$ with $(\nabla_1^2+a^2)U=0$ where U is plane tiling function. Hence (35)-(37) reduces to the following system of equations

$$2(D^2-a^2)^2W-\frac{R^{1/2}a^2}{\sqrt{\lambda_1}}(1+\lambda_1 f_T(z))\Theta+\frac{Rs^{1/2}a^2}{\sqrt{\lambda_2}}(1-\lambda_2 f_C(z))\Phi=0 \tag{38}$$

$$2(D^2-a^2)\Theta+\frac{R^{1/2}}{\sqrt{\lambda_1}}(1+\lambda_1 f_T(z))W+\sqrt{\frac{\lambda_2}{\lambda_1}}h\Phi=0 \tag{39}$$

$$2(D^2-a^2-\eta)\Phi-\frac{Rs^{1/2}}{\sqrt{\lambda_2}}(1-\lambda_2 f_C(z))W+\sqrt{\frac{\lambda_2}{\lambda_1}}h\Theta=0 \tag{40}$$

The corresponding boundary conditions are

$$W=DW=\Theta=\Phi=0 \quad \text{at } z=0,1 \tag{41}$$

The value of critical Rayleigh number $R_{cE}=\max_{\lambda_1\lambda_2}\min_a R(\lambda_1,\lambda_2,a)$ is obtained by eigenvalue problem (38)-(40) with boundary condition (41). The system is solved using Galerkin technique as described in section 3.

5. Results and discussion section

The numerical calculations are carried out to see the impact of different temperature and concentration gradient profiles. To this end, the linear, parabolic, inverted parabolic, piecewise linear, oscillatory and stepwise profiles are considered. The critical Rayleigh number (R_{cL}) for linear theory and critical Rayleigh number (R_{cE}) for non-linear theory are calculated and compared to see the possibility of existence of subcritical instability. In order to validate the numerical scheme, the results are calculated for a model not containing solute ($Rs=0, h=0, \eta=0$). Results

are found to be in good agreement with Currie [26] in case of piecewise profile $(0<\xi<1)$ and linear profile $(\xi=1)$ (Figure 2 and Table 1) and with Sparrow et al. [24] for parabolic profile (Table 2).

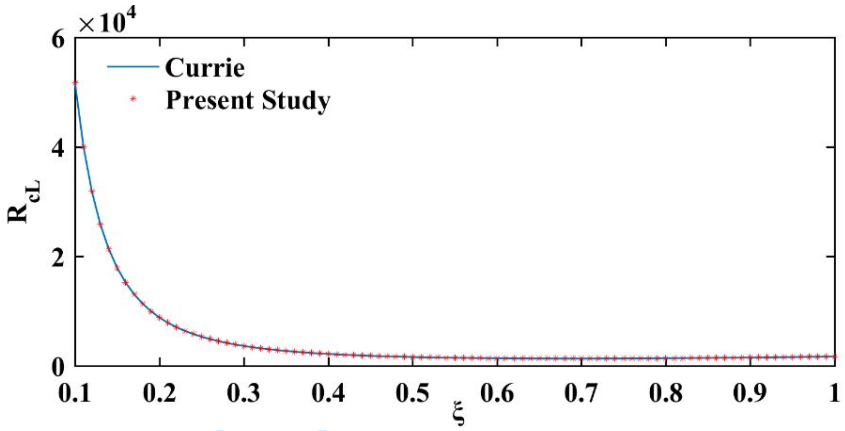

Figure 2: Validation of the results with Currie [26] for the piecewise profile $(0<\xi<1)$ and linear profile $(\xi=1)$.

Table 1: Comparison of present study with Currie [26]

	Currie [26]		**Present study**		
	ξ	R_{cL}	ξ	R_{cL}	R_{cE}
Piecewise Profile	0.72	1340	0.70	1347.89	1339.07
Linear Profile	1	1707.8	1	1707.76	1707.76

Table 2: Comparison of present study for parabolic profile

Sparrow et al. [24]		**Present study**	
a_{cL}	R_{cL}	a_{cL}	R_{cL}
3.13	1694.953	3.13	1694.9936

5.1 Linear temperature and concentration profiles

For the linear temperature and concentration profiles the gradient functions are

$$f_T(z)=f_C(z)=1$$

From the numerical calculations, it is observed that the increase in the values of solute Rayleigh number delays the onset of convection (Figure 3 and Table 3). The stability boundary obtained by non-linear theory is found to be unaffected by the solute Rayleigh number and reaction parameters.

When $Rs = 0$ the results of linear and non-linear analyses coincide, however, existence of subcritical region of instability is noted in the presence of solute Rayleigh number. It is also observed that the reaction parameters h and η have counter-effect on the onset of convection. Increase in value of h for fixed η delays the onset of convection while increase in value of η for fixed h hastens the onset of convection. An increase in h value promotes the dissolution reaction to absorb some of the heat energy causing the surrounding environment to feel cold. The net result is that a larger temperature gradient is required for the onset of convection and hence system is stabilized. For a fixed h, increase in the value of η corresponds to a faster rate of chemical reaction that results in negligible diffusion of salt component and provides an early onset of convection. When both h and η, varies at the same rate the two opposing forces try to counter balance the effect, however, due to larger solubility the onset of convection is delayed slightly. Thus the value of the critical Rayleigh number R_{cL} obtained at $h = \eta = 1$ is above the value of R_{cL} at $h = \eta = 0$. It is not always necessary that linear instability threshold coincide with the energy threshold but when the system is symmetric then linear instability theory always represents accurately the onset of convection. In Figure 3, subcritical instability exists i.e. linear instability theory is unable to capture the physics for the onset because of the two sources of anti-symmetry, the terms of Rs and the terms of h.

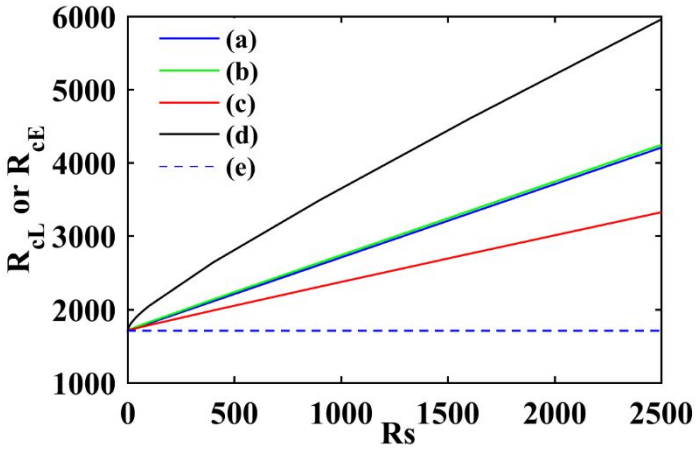

Figure 3: Variation of critical Rayleigh numbers R_{cL} (linear analysis) and R_{cE} (nonlinear analysis) with solute Rayleigh number Rs for linear model $\left[f_T(z) = f_C(z) = 1 \right]$. Solid lines (—) are results for linear analysis and dashed line (---) is result of nonlinear analysis. For linear analysis, curve (a) is for $h = \eta = 0$, curve (b) is for $h = \eta = 1$, curve (c) is for $h = 1, \eta = 12$, and curve (d) is for $h = 12, \eta = 1$. From the nonlinear analysis, curve (e) is drawn for $h = \eta = 0$. It is also noted that the curve (e) is unchanged for varying h and η. This can be seen in Table 3.

Table 3: Variation of critical Rayleigh number (R_{cL}, R_{cE}) with solute Rayleigh number Rs and chemical reaction parameters (h, η) for the linear profile.

	$(Rs)^{1/2}$	R_{cL}	a_{cL}	R_{cE}	a_{cE}	λ_1	λ_2
$h=\eta=0$	0	1707.764	3.12	1707.764	3.12	1	--
	10	1807.763	3.12	1707.764	3.12	1	1
	20	2107.765	3.12	1707.764	3.12	1	1
	30	2607.757	3.12	1707.764	3.12	1	1
	40	3307.757	3.12	1707.764	3.12	1	1
	50	4207.754	3.12	1707.764	3.12	1	1
	60	5307.764	3.12	1707.764	3.12	1	1
	70	6607.755	3.12	1707.764	3.12	1	1
	80	8107.76	3.12	1707.764	3.12	1	1
	90	9807.753	3.12	1707.764	3.12	1	1
	100	11707.76	3.12	1707.764	3.12	1	1
$h=\eta=1$	0	1707.764	3.12	1707.764	3.12	1	--
	10	1823.572	3.13	1707.764	3.12	1	0.83
	20	2133.054	3.13	1707.764	3.12	1	0.90
	30	2638.713	3.13	1707.764	3.12	1	0.93
	40	3342.146	3.14	1707.764	3.12	1	0.95
	50	4244.314	3.14	1707.764	3.12	1	0.96
	60	5345.73	3.14	1707.764	3.12	1	0.97
	70	6679.335	3.14	1707.764	3.12	1	0.97
	80	8147.373	3.14	1707.764	3.12	1	0.97
	90	9847.863	3.14	1707.764	3.12	1	0.98
	100	11748.22	3.14	1707.764	3.12	1	0.98
$h=1, \eta=12$	0	1707.764	3.12	1707.764	3.12	1	--
	10	1783.187	3.11	1707.764	3.12	1	0.83
	20	1983.776	3.07	1707.764	3.12	1	0.91
	30	2309.043	3.00	1707.764	3.12	1	0.93
	40	2757.111	2.92	1707.764	3.12	1	0.95
	50	3325.102	2.81	1707.764	3.12	1	0.96
	60	4009.448	2.70	1707.764	3.12	1	0.97
	70	4806.496	2.58	1707.764	3.12	1	0.97
	80	5712.881	2.47	1707.764	3.12	1	0.97
	90	6725.689	2.35	1707.764	3.12	1	0.98
	100	7842.661	2.25	1707.764	3.12	1	0.98

5.2 Parabolic and inverted parabolic temperature and concentration profiles

For the parabolic temperature and concentration profiles, the gradient functions are

$$f_T(z) = f_C(z) = 2z$$

and for the inverted parabolic temperature and concentration profiles the gradient functions are

$$f_T(z) = f_C(z) = 2(1-z)$$

We begin the discussion by noting that the results of linear and non-linear analysis do not coincide even for the case when solute is absent. In (Figure 4a, Table 4), it is found from numerical calculation that for both parabolic and inverted parabolic profile the onset of convection occurs at same values of critical Rayleigh number. It is also noted that the onset of convection for these profiles occur at slightly lower values of Rayleigh number when compared with linear profile. The increase in the values of solute Rayleigh number Rs delays the onset of convection, that is, the critical values of Rayleigh number increases with increase in Rs values. However, it was interesting to note that stability region obtained due to finite perturbation decreases with the increase in Rs values for these profiles. Moreover, the subcritical instability region increases with the increase in Rayleigh number of solute. In Figure 4a, the stability boundary obtained by nonlinear analysis is plotted only with $h = \eta = 0$.The results of other values of h and η are so close to the $h = \eta = 0$ that they seemed overlapped.To visualize the difference in results of energy theory the Figure 4b is presented.The stability boundaries when Rs increases, are influenced by the chemical reaction parameters. The stability region increases in the presence of chemical reaction. Due to the closeness in stability boundaries the plots in the following subsections are presented by considering stability boundaries at $h = \eta = 0$.

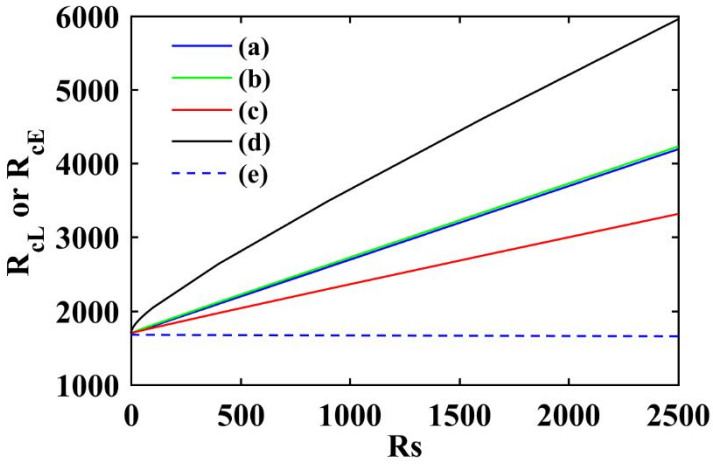

Figure 4a: Variation of critical Rayleigh numbers (R_{cL}, R_{cE}) with solute Rayleigh number Rs for the case of parabolic profile. Solid lines (—) are results for linear analysis and dashed line (---) is result of nonlinear analysis. For linear analysis, curve (a) is for $h = \eta = 0$, curve (b) is for $h = \eta = 1$, curve (c) is for $h = 1, \eta = 12$, and curve (d) is for $h = 12, \eta = 1$. From the nonlinear analysis, curve (e) is drawn for $h = \eta = 0$.

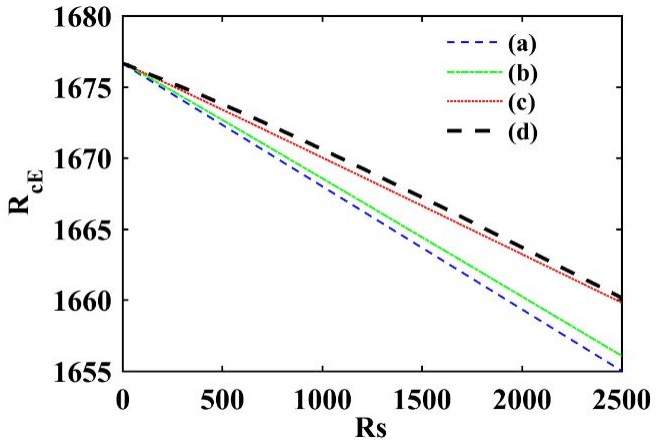

Figure 4b: Variation of critical Rayleigh number R_{cE} with solute Rayleigh number Rs using nonlinear analysis for the case of parabolic profile with (a) $h = \eta = 0$, (b) $h = \eta = 1$, (c) $h = 1, \eta = 12$, (d) $h = 12, \eta = 1$. It is observed that stability threshold increases with reaction parameters h, η and decreases with solute Rayleigh number Rs.

Table 4: Variation of critical Rayleigh numbers (R_{cL}, R_{cE}) with solute Rayleigh number Rs and chemical reaction parameters (h, η) for parabolic profile (or inverted parabolic profile).

	$(Rs)^{1/2}$	R_{cL}	a_{cL}	R_{cE}	a_{cE}	λ_1	λ_2
$h=\eta=0$	0	1694.994	3.13	1676.681	3.13	0.96	--
	10	1794.988	3.13	1675.83	3.13	0.96	0.96
	20	2094.994	3.13	1673.293	3.13	0.96	0.96
	30	2594.996	3.13	1668.943	3.14	0.96	0.96
	40	3294.99	3.13	1662.902	3.13	0.96	0.96
	50	4194.984	3.13	1655.115	3.14	0.96	0.96
	60	5294.993	3.13	1645.6	3.14	0.97	0.97
	70	6594.983	3.13	1634.31	3.15	0.97	0.97
	80	8094.979	3.13	1621.262	3.15	0.97	0.97
	90	9794.982	3.13	1606.414	3.16	0.97	0.97
	100	11694.99	3.13	1589.776	3.17	0.97	0.97
$h=\eta=1$	0	1694.994	3.13	1676.681	3.13	0.96	--
	10	1810.613	3.14	1675.953	3.13	0.96	0.80
	20	2119.958	3.14	1673.546	3.13	0.96	0.88
	30	2625.527	3.15	1669.458	3.14	0.96	0.90
	40	3328.898	3.15	1663.669	3.14	0.96	0.92
	50	4231.021	3.15	1656.181	3.14	0.96	0.93
	60	5332.402	3.15	1646.972	3.14	0.97	0.93
	70	6633.353	3.15	1636.049	3.15	0.97	0.94
	80	8134.002	3.15	1623.389	3.15	0.97	0.94
	90	9834.491	3.15	1608.948	3.15	0.97	0.94
	100	11734.85	3.15	1592.832	3.15	0.97	0.95
$h=1, \eta=12$	0	1694.994	3.12	1676.681	3.13	0.96	--
	10	1770.508	3.12	1676.084	3.13	0.96	0.80
	20	1971.609	3.08	1674.119	3.13	0.96	0.87
	30	2297.764	3.01	1670.774	3.13	0.96	0.90
	40	2747.07	2.92	1666.027	3.14	0.96	0.91
	50	3316.516	2.82	1659.902	3.14	0.96	0.92
	60	4002.536	2.70	1652.374	3.14	0.96	0.93
	70	4801.409	2.58	1643.427	3.15	0.96	0.94
	80	5710.628	2.47	1633.065	3.15	0.96	0.94
	90	6724.607	2.35	1621.294	3.16	0.96	0.94
	100	7843.777	2.25	1608.066	3.16	0.97	0.94

5.3 Piecewise linear temperature and concentration profiles

For the piecewise linear temperature and concentration profiles, the temperature and solute gradients are

$$f_T(z) = f_C(z) = \begin{cases} \dfrac{1}{\xi}, & 0 \le z < \xi, \\ 0, & \xi < z \le 1 \end{cases}$$

where ξ is the thermal or concentration depth parameter ranging from 0 to 1.

It is observed from Figure 5a that as ξ increases from 0 to 1 the values of critical Rayleigh numbers (R_{cL}, R_{cE}) first decreases to a minimum value and then starts increasing. The minimum value is obtained at $\xi = 0.7$ which agrees closely to the value $\xi = 0.72$ obtained by Currie [22] for the model of sudden heating from below. At $\xi = 0.7$, the critical values of Rayleigh numbers (R_{cL}, R_{cE}) are lower than at $\xi = 1$, which means that the onset of convection is early in piecewise profile as compared to linear profile and the region of stability has decreased. The effect of increase in the values of solute Rayleigh number Rs on onset of convection is delayed (Table 5 and Figure 5b) however, the region of stability is decreasing and region of subcritical instability is growing.

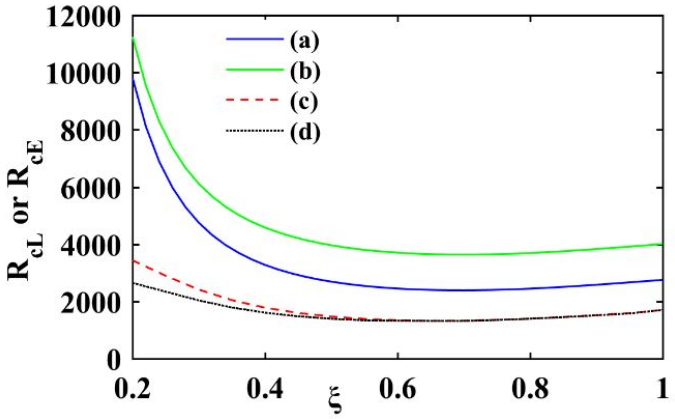

Figure 5a: Variation of critical Rayleigh numbers (R_{cL}, R_{cE}) with depth parameter (ξ) for the case of piecewise profile. Solid lines are results of linear analysis and dashed lines are results of nonlinear analysis. For linear analysis, curve (a) is for $Rs = 1600, h = 1, \eta = 12$, curve (b) is for $Rs = 3600, h = 1, \eta = 12$, From the nonlinear analysis, curve (c) is for $Rs = 1600, h = 1, \eta = 12$ and curve (d) is for $Rs = 3600, h = 1, \eta = 12$.

Table 5: Variation of critical Rayleigh numbers (R_{cL}, R_{cE}) with solute Rayleigh number Rs and chemical reaction parameters (h,η) in case of piecewise linear profile at critical value of thermal or concentration depth $\xi_c = 0.7$.

	$(Rs)^{1/2}$	R_{cL}	a_{cL}	R_{cE}	a_{cE}	λ_1	λ_2
$h=\eta=0$	0	1347.896	3.12	1339.07	3.12	0.78	--
	10	1447.894	3.12	1338.557	3.12	0.78	0.78
	20	1747.892	3.12	1337.014	3.12	0.78	0.78
	30	2247.888	3.12	1334.441	3.13	0.78	0.78
	40	2947.893	3.12	1330.82	3.13	0.78	0.78
	50	3847.895	3.12	1326.14	3.13	0.78	0.78
	60	4947.884	3.12	1320.385	3.13	0.78	0.78
	70	6247.891	3.12	1313.526	3.14	0.78	0.78
	80	7747.89	3.12	1305.536	3.14	0.78	0.78
	90	9447.879	3.12	1296.382	3.14	0.78	0.78
	100	11347.9	3.12	1286.001	3.15	0.78	0.78
$h=\eta=1$	0	1347.896	3.12	1339.07	3.12	0.78	--
	10	1461.441	3.13	1338.652	3.12	0.78	0.66
	20	1769.052	3.14	1337.248	3.12	0.78	0.71
	30	2273.306	3.14	1334.828	3.13	0.78	0.73
	40	2975.779	3.14	1331.374	3.13	0.78	0.74
	50	3877.266	3.14	1326.89	3.13	0.78	0.75
	60	4978.234	3.14	1321.308	3.13	0.78	0.76
	70	6278.867	3.14	1314.701	3.14	0.78	0.76
	80	7779.311	3.14	1306.953	3.14	0.78	0.76
	90	9479.632	3.14	1298.017	3.15	0.78	0.76
	100	11594.21	3.14	1287.92	3.15	0.78	0.77
$h=1,\eta=12$	0	1347.896	3.12	1339.07	3.12	0.78	--
	10	1422.052	3.11	1338.718	3.12	0.78	0.65
	20	1621.818	3.06	1337.54	3.12	0.78	0.71
	30	1946.336	2.98	1335.508	3.14	0.78	0.73
	40	2393.098	2.87	1332.615	3.14	0.78	0.73
	50	2958.457	2.75	1328.836	3.14	0.78	0.74
	60	3638.273	2.61	1324.196	3.14	0.78	0.75
	70	4428.596	2.48	1319.346	3.14	0.78	0.75
	80	5326.095	2.35	1312.142	3.14	0.78	0.76
	90	6328.155	2.24	1304.741	3.15	0.78	0.76
	100	7432.819	2.13	1296.324	3.15	0.78	0.76

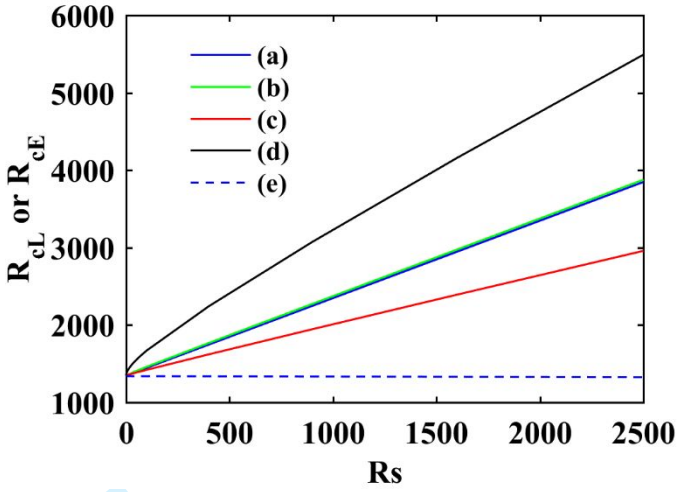

Figure 5b: Variation of critical Rayleigh numbers (R_{cL}, R_{cE}) with solute Rayleigh number Rs for the case of piecewisewise linear profile. Solid lines (—) are results of linear analysis and dashed line (---) is result of nonlinear analysis. For linear analysis, curve (a) is for $h = \eta = 0$, curve (b) is for $h = \eta = 1$, curve (c) is for $h = 1, \eta = 12$, and curve (d) is for $h = 12, \eta = 1$. From the nonlinear analysis, curve (e) is drawn for $h = \eta = 0$.

5.4 Oscillatory profiles for temperature and concentration gradients

For the oscillatory temperature and concentration profiles, the gradients functions are

$$f_T(z) = f_C(z) = \frac{\pi}{2}\sin(\pi z)$$

In the Figure 6 and Table 6, the variation of critical Rayleigh numbers (R_{cL}, R_{cE}) against solute Rayleigh number Rs for the different values of chemical reaction parameters h and η are presented. It is observed that the stabilizing effect of solute Rayleigh number Rs and behavior of chemical reaction parameters h, η on the onset of convection continues to hold on the same lines as in the other assumed temperature and concentration profiles. The oscillatory profile is observed to be more unstable than the linear, parabolic, inverted parabolic, and piecewise linear profiles as the critical value of Rayleigh number R_{cL} is found to be less for oscillatory profile when compared to these profiles. It is also observed that the subcritical region of instability increases with increase in Rs parameter. As like the other assumed profiles of temperature and concentration gradients, an increase in the h values (for fixed values of η) delays the onset of convection however, an increase in η values (for fixed values of h) hastens the onset of convection.

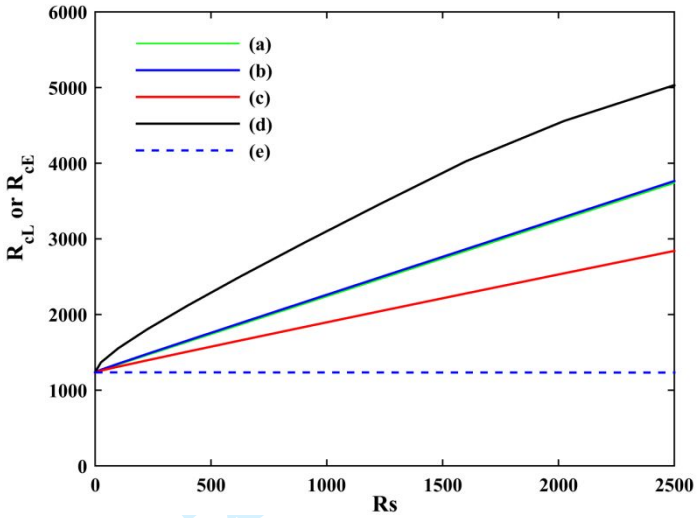

Figure 6: Variation of critical Rayleigh numbers (R_{cL}, R_{cE}) with solute Rayleigh number Rs for the case of oscillatory profiles of temperature and concentration gradients. Solid lines (—) are results of linear analysis and dashed line (---) is result of nonlinear analysis. For linear analysis, curve (a) is for $h = \eta = 0$, curve (b) is for $h = \eta = 1$, curve (c) is for $h = 1, \eta = 12$, and curve (d) is for $h = 12, \eta = 1$. From the nonlinear analysis, curve (e) is drawn for $h = \eta = 0$.

Table 6: Variation of critical Rayleigh numbers (R_{cL}, R_{cE}) with solute Rayleigh number Rs for chemical reaction parameters (h,η) in case of oscillatory profiles of temperature and concentration gradients.

	$(Rs)^{1/2}$	R_{cL}	a_{cL}	R_{cE}	a_{cE}	λ_1	λ_2
$h=\eta=0$	0	1237.561	3.11	1235.8839	3.11	0.72	--
	10	1337.558	3.11	1235.7771	3.11	0.72	0.72
	20	1637.561	3.11	1235.4566	3.11	0.72	0.72
	30	2137.561	3.11	1234.9223	3.11	0.72	0.72
	40	2837.56	3.11	1234.1741	3.11	0.72	0.72
	50	3737.618	3.11	1233.2116	3.11	0.72	0.72
	60	4837.473	3.11	1232.0345	3.11	0.72	0.72
	70	6137.561	3.11	1231.3125	3.11	0.72	0.72
	80	7637.594	3.11	1230.3345	3.11	0.72	0.72
	90	9337.559	3.11	1227.2131	3.12	0.72	0.72
	100	11237.56	3.11	1225.1710	3.12	0.72	0.72
$h=\eta=1$	0	1237.561	3.11	1235.8812	3.12	0.72	--
	10	1350.446	3.12	1235.8148	3.12	0.72	0.66
	20	1657.499	3.13	1235.5415	3.12	0.72	0.68
	30	2161.365	3.13	1235.0603	3.13	0.72	0.70
	40	2863.558	3.13	1234.3121	3.13	0.72	0.70
	50	3764.935	3.13	1233.4578	3.13	0.72	0.70
	60	4865.62	3.13	1232.3439	3.13	0.72	0.71
	70	6166.255	3.14	1230.9696	3.14	0.72	0.71
	80	7666.696	3.14	1229.4479	3.14	0.72	0.71
	90	9366.908	3.14	1227.7127	3.15	0.72	0.71
	100	11267.11	3.14	1225.7586	3.15	0.72	0.71
$h=1,\eta=12$	0	1237.561	3.11	1235.8812	3.11	0.72	--
	10	1311.173	3.10	1235.4190	3.11	0.72	0.65
	20	1510.113	3.05	1235.5782	3.11	0.72	0.66
	30	1833.407	2.96	1235.1461	3.11	0.72	0.68
	40	2278.32	2.85	1234.5241	3.11	0.72	0.68
	50	2840.965	2.78	1233.6991	3.11	0.72	0.69
	60	3517.009	2.65	1232.7107	3.11	0.72	0.70
	70	4302.45	2.51	1231.5054	3.11	0.72	0.71
	80	5194.021	2.37	1230.0869	3.11	0.72	0.71
	90	6189.266	2.19	1228.5363	3.12	0.72	0.71
	100	7286.368	2.09	1226.7869	3.12	0.72	0.71

5.5 Step function profile

The step profiles occurs when there is superposition of two layers and basic temperature (or concentration) drops suddenly by an amount of ΔT (or ΔC) at $z = \xi$ given by

$$f_T(z) = f_C(z) = \delta(z - \xi)$$

where δ is Dirac delta function and ξ is thermal or concentration depth parameter varying from 0 to 1.

The variation of ξ from 0 to 1 was made and critical Rayleigh numbers are calculated and it is found that the system is most unstable when $\xi = 0.5$. Numerical values are presented in Table 7 and Figure 7 for fixed value of $\xi = 0.5$ and increasing solute Rayleigh number Rs which confirms the early onset of convection as compared to the profiles discussed earlier. The result is also true for fixed Rs and varying chemical reaction parameters. Stabilty region reduces with increase in Rs values and this behaviour is found to be consistent in all the profiles of temperature and concentration gradients.

In Figure 8(a-d), the comparison of piecewise and stepwise profile is made for increasing value of ξ and for different values of solute Rayleigh number Rs and chemical reaction parameters h, η. It is evident from all figures that as ξ varies from 0 to 1 the critical Rayleigh number first decreases to a minimum value and then starts increasing. In all cases, the minimum value of Rayleigh number is attained at $\xi = 0.5$ for stepwise profile and at $\xi = 0.7$ for the piecewise profile. As $\xi \to 1$, the critical Rayleigh number attains a finite value for piecewise profile while it tends to infinite for stepwise profile. For the piecewise profile as ξ becomes 1, the profile becomes linear and results match with the results of linear profile model. For the stepwise profile as ξ becomes 1, the two superposed layers become a single layer with constant temperature and so the system is always stable leading to the critical Rayleigh number values tending to infinity.

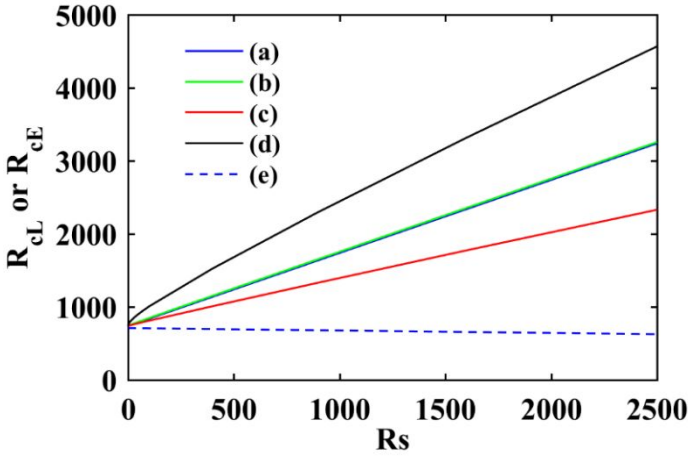

Figure 7: Variation of critical Rayleigh numbers (R_{cL}, R_{cE}) with solute Rayleigh number Rs for the case of stepwise profile. Solid lines (—) are results of linear analysis and dashed line (---) is result of nonlinear analysis. For linear analysis, curve (a) is for $h = \eta = 0$, curve (b) is for $h = \eta = 1$, curve (c) is for $h = 1, \eta = 12$, and curve (d) is for $h = 12, \eta = 1$. From the nonlinear analysis, curve (e) is drawn for $h = \eta = 0$.

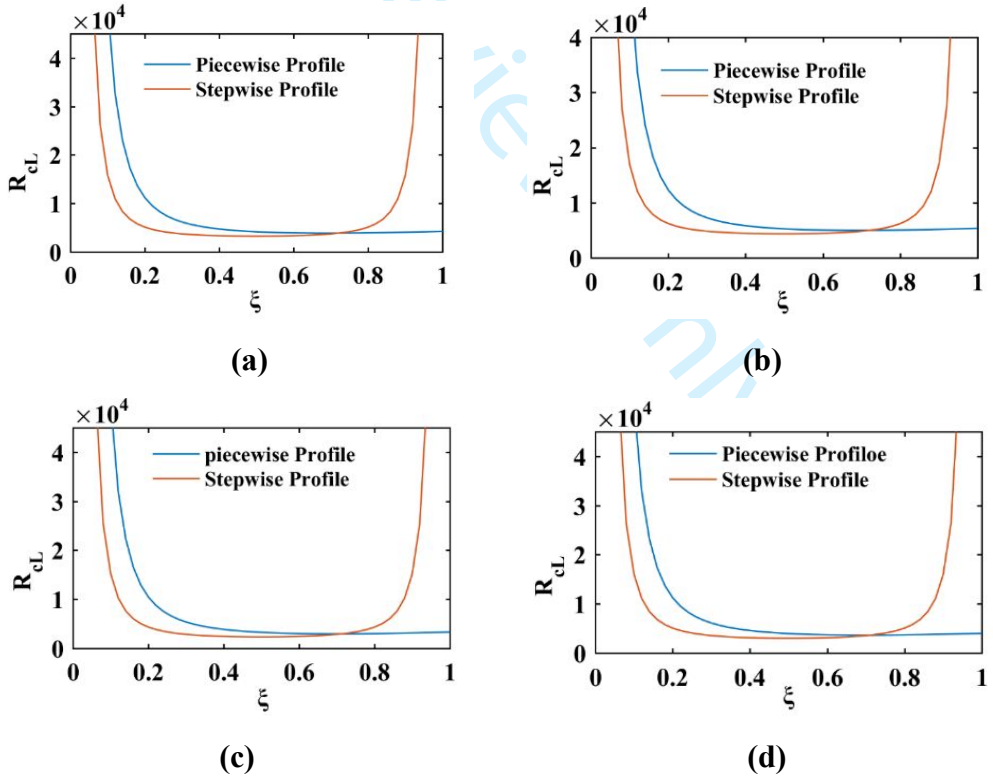

Figure 8: Comparison of Piecewise and stepwise profiles with variation in depth parameter (ξ) at $h = 1$, and (a) $Rs = 2500, \eta = 1$, (b) $Rs = 3600, \eta = 1$, (c) $Rs = 2500, \eta = 12$, (d) $Rs = 3600, \eta = 12$

.

Table 7: Variation of critical Rayleigh numbers (R_{cL}, R_{cE}) with solute Rayleigh number Rs and chemical reaction parameters (h,η) in case of step profile functions at critical value of thermal or concentration depth $\xi_c = 0.5$.

	$(Rs)^{1/2}$	R_{aL}	a_{cL}	R_{cE}	a_{cE}	λ_1	λ_2
$h=\eta=0$	0	739.9706	3.12	709.6416	3.15	0.40	--
	10	839.9679	3.12	706.4007	3.16	0.40	0.40
	20	1139.967	3.12	696.6274	3.17	0.40	0.40
	30	1639.967	3.12	680.2446	3.19	0.40	0.40
	40	2339.966	3.12	657.0814	3.21	0.40	0.40
	50	3239.966	3.12	626.8964	3.25	0.40	0.40
	60	4339.964	3.12	589.3533	3.30	0.40	0.40
	70	5639.965	3.12	543.967	3.36	0.40	0.40
	80	7139.963	3.12	490.0733	3.44	0.40	0.40
	90	8839.967	3.12	426.7612	3.53	0.40	0.40
	100	10739.96	3.12	352.7335	3.65	0.40	0.40
$h=\eta=1$	0	739.9706	3.12	709.6416	3.15	0.40	--
	10	848.9823	3.13	706.842	3.16	0.40	0.35
	20	1153.098	3.14	697.6254	3.17	0.40	0.37
	30	1655.033	3.14	681.8731	3.19	0.40	0.38
	40	2356.025	3.14	658.8308	3.22	0.40	0.40
	50	3256.574	3.14	629.3977	3.25	0.40	0.40
	60	4356.911	3.14	592.6985	3.30	0.40	0.40
	70	5657.116	3.15	548.2622	3.37	0.40	0.40
	80	7157.262	3.15	495.4408	3.44	0.40	0.40
	90	8857.37	3.15	425.0566	3.54	0.40	0.40
	100	10757.44	3.15	360.6847	3.65	0.40	0.40
$h=1,\eta=12$	0	739.9706	3.12	709.3913	3.15	0.40	--
	10	811.6687	3.09	707.1345	3.16	0.40	0.34
	20	1009.994	3.00	698.9203	3.16	0.40	0.36
	30	1332.557	2.86	685.8166	3.19	0.40	0.38
	40	1774.617	2.69	664.7889	3.21	0.40	0.38
	50	2330.63	2.51	638.6437	3.24	0.40	0.38
	60	2995.69	2.34	605.5094	3.29	0.40	0.39
	70	3766.191	2.19	564.4806	3.34	0.40	0.39
	80	4639.694	2.05	517.5443	3.42	0.40	0.39
	90	5614.67	1.94	462.7532	3.47	0.40	0.39
	100	6690.095	1.83	399.2244	3.62	0.40	0.40

The neutral stability curves are drawn for linear, parabolic, piecewise linear profile, oscillatory profile, and stepwise profiles, of temperature and concentration gradients using linear analysis [Figure 9(a), Figure 10(a)] and nonlinear stability analysis [Figure 9(b), Figure 10(b)]. The critical values of Rayleigh number R_{cL} obtained using linear theory correspond to the onset of convection and from Figure 9(a) and 10(a), it is seen that convection occurs for stepwise profile at much lower values of critical Rayleigh number when compared to the other assumed profiles of temperature and concentration gradients. The critical values of Rayleigh number R_{cE} obtained by nonlinear analysis provide the stability threshold and from Figure 9(b) and 10(b) it is observed that linear profile is much stable in compared to the other considered profiles of temperature and concentration gradients . It is also observed that with the increase in h values the onset of convection is delayed, however, the stability region is marginally shifted which results in increase in region of subcritical instability.

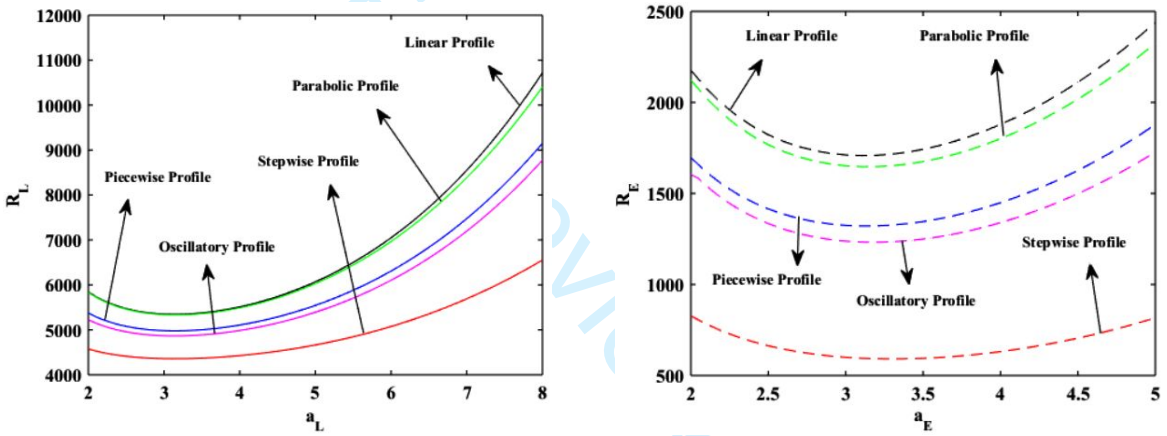

(a) (b)

Figure 9: Neutral stability curves for fixed value of $Rs = 3600, h = 1, \eta = 1$, (a) linear theory, and (b) nonlinear stability analysis.

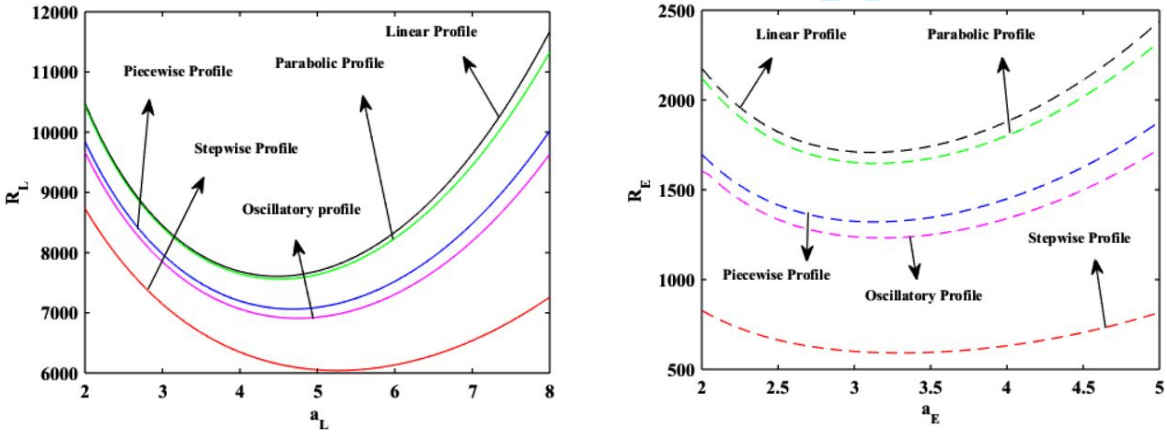

(a) (b)

Figure 10: Neutral stability curves for fixed value of $Rs = 3600, h = 12, \eta = 1$, (a) linear theory, and (b) nonlinear stability analysis.

6. Conclusions

In this work, the effect of different temperature and concentration profiles on the stability of layer of fluid with chemical reaction is analyzed. It is observed that the parabolic and inverted parabolic profiles have same effect on the stability of system, and the onset of convection for both profiles occur at a slightly lower values as compared to the linear profile. It is found that the stepwise profile is most unstable followed by the oscillatory profile being the second most unstable. The solute Rayleigh number Rs has stabilizing effect on the onset of convection. The effect of chemical reaction parameter h is stabilizing while the parameter η is destabilizing. For all considered profiles, the region of subcritical instability exists.

Acknowledgement

One of the authors, Vinit Kumar Tripathi gratefully acknowledges the financial assistance received from NIT Delhi.

References

[1] S. Chandrasekhar, Hydrodynamic and hydromantic stability, Dover, New York (1981).

[2] H.E. Huppert, J.S. Turner, J. Fluid Mech., 106 (1981).

[3] D.J. Wollkind, H.L. Frisch, Phys. Fluids, 14(1), 13 (1971).

[4] D.J. Wollkind, H.L. Frisch, Phys. Fluids, 14(3), 482 (1971).

[5] J. Bdzil, H.L. Frisch, Phys. Fluids, 14(3), 475 (1971).

[6] J. Bdzil, H.L. Frisch, J. Chem. Phys., 72(3), 1875 (1980).

[7] D. kowiczKrusin, J. Ross, J. Chem. Phys., 72, 3577 (1980).

[8] M. Gitterman, V. Steinberg, Phys. Fluids, 26, 393 (1983).

[9] V. Steinberg, H.R. Brand, J. Chem. Phys., 80(1), 431 (1984).

[10] D. Pritchard, C.N. Richardson, J. Fluid Mech., 571, 59 (2007).

[11] S. Wang, W. Tan, Phys. Lett. A, 373(A), 776 (2009).

[12] A.K. Srivastava, P. Bera, Transp. Porous Media, 97, 161 (2013).

[13] M.S. Malashetty, B.S. Biradar, Phys. Fluids, 23, 064102 (2011)

[14] B.Al. Sulaimi**,** Int. J. Heat Mass Transf., 86, 369 (2015).

[15] B.Al. Sulaimi, Ric. Mat., 65, 381 (2016).

[16] A.J. Harfash, G.A. Meften, Appl. Math. Comput., 341, 301 (2019).

[17] O.D. Makinde, Int. J. Numer. Meth. Fl., 59, 791 (2009).

[18] O.D. Makinde, Math. Comput. Model., 37(3-4), 251 (2003).

[19] O.D. Makinde, P.Y. Mhone, Comput Math. Appl., 53(1), 128 (2007).

[20] O.D. Makinde, P.Y. Mhone, Flow Turbul. Combust, 83, 21 (2009).

[21] A. Graham, Philos. Trans. R. Soc. A, 232, 285 (1933).

[22] K. Chandra, P. Roy. Soc. A-Math. Phy., 164, 231 (1938).

[23] O.G. Sutton, P. Roy. Soc. A-Math. Phy., 204, 297 (1950).
[24] E.M. Sparrow, R.J. Goldstein, V.K. Jonsson, J. Fluid Mech., 18, 513-528 (1964).
[25] G.M. Homsy, J. Fluid Mech., 60, 129 (1973).
[26] I.G. Currie, J. Fluid Mech., 29, 337 (1967).
[27] D.A. Nield, J. Fluid Mech., 71(3), 454 (1975).
[28] N. Rudraiah, B. Veerappa, B.S. Rao, J. Heat Transfer, 102, 254 (1980).
[29] I.S. Shivakumara, Arch. Appl. Mech., 80, 949 (2010).
[30] B. Straughan, The energy method, stability and non-linear convection, Springer science, 91 (2013).
[31] D.D. Joseph, Arch. Ration. Mech. Anal., 20, 59 (1965).